Noninvasive assessment of testicular torsion in rabbits using frequency-domain near-infrared spectroscopy: prospects for pediatric urology

Bertan Hallacoglu*
Richard S. Matulewicz*
Tufts University
Department of Biomedical Engineering
4 Colby Street
Medford, Massachusetts 02155

Harriet J. Paltiel
Horacio Padua
Children's Hospital Boston
Department of Radiology
300 Longwood Avenue
Boston, Massachusetts 02115

Patricio Gargollo
Glenn Cannon
Children's Hospital Boston
Department of Urology
300 Longwood Avenue
Boston, Massachusetts 02115

Ahmad Alomari
Children's Hospital Boston
Department of Radiology
300 Longwood Avenue
Boston, Massachusetts 02115

Angelo Sassaroli
Sergio Fantini†
Tufts University
Department of Biomedical Engineering
4 Colby Street
Medford, Massachusetts 02155

Abstract. We present a quantitative near-IR spectroscopy study of the absolute values of oxygen saturation of hemoglobin before and after surgically induced testicular torsion in adult rabbits. Unilateral testicular torsions (0, 540, or 720 deg) on experimental testes and contralateral sham surgery on control testes are performed in four adult rabbits. A specially designed optical probe for measurements at multiple source-detector distances and a commercial frequency-domain tissue spectrometer are used to measure absolute values of testicular hemoglobin saturation. Our results show: (1) a consistent baseline absolute tissue hemoglobin saturation value of 78±5%, (2) a comparable tissue hemoglobin saturation of 77±6% after sham surgery, and (3) a significantly lower tissue hemoglobin saturation of 36±2% after 540- and 720-deg testicular torsion surgery. Our findings demonstrate the feasibility of performing frequency-domain, multidistance near-IR spectroscopy for absolute testicular oximetry in the assessment of testicular torsion. We conclude that near-IR spectroscopy has potential to serve as a clinical diagnostic and monitoring tool for the assessment of absolute testicular hemoglobin desaturation caused by torsion, with the possibility of serving as a complement to conventional color and spectral Doppler ultrasonography. [DOI: 10.1117/1.3253318]

Keywords: near-infrared spectroscopy; testicular torsion; absolute tissue oximetry.

Paper 09021R received Jan. 22, 2009; revised manuscript received Jul. 16, 2009; accepted for publication Aug. 11, 2009; published online Oct. 28, 2009.

1 Introduction

Quantification of absolute or relative concentrations of chromophores in tissues through spectroscopic measurements of near-IR diffuse reflectance is an established method in the noninvasive examination of biological tissues.[1] Research in this area has led to applications that focused on different types of tissues such as brain[2] (for monitoring hemodynamics associated with brain activation), skeletal muscles[3] (for studying muscle metabolism), and the breast[4] (for tumor detection), all indicative of the versatility and broad potential of near-IR spectroscopy (NIRS) to obtain physiological and diagnostic information from various tissues within the body.

In this paper, we explore the potential of NIRS in pediatric urology, specifically in the detection, assessment, and evaluation of testicular torsion. Testicular torsion is the most serious cause of acute scrotal symptoms, with an incidence[5] of approximately 1 in 4000. Torsion occurs at all ages, although it is most common in the pediatric population. Because of the risk of infarction, testicular torsion must be immediately excluded in any patient who presents with acute scrotal symptoms. Historically, about 50% of all torsive testes explored emergently are successfully salvaged, while the other 50% require orchiectomy or develop postoperative atrophy.[6] Color Doppler ultrasound (US) is routinely employed worldwide to elucidate the various causes of acute scrotal pain with a high degree of success due to its ability to directly visualize the testicular blood supply and to depict alterations in perfusion without the need for ionizing radiation. However, there are

*These authors contributed equally to this article.
†Address all correspondence to: Sergio Fantini, Tufts University, Department of Biomedical Engineering, 4 Colby Street, Medford, MA 02155. Tel.: 617-627-4356; E-mail: Sergio.Fantini@tufts.edu

1083-3668/2009/14(5)/054027/7/$25.00 © 2009 SPIE

persistent limitations of conventional color Doppler US in the diagnosis of testicular torsion, especially in the pediatric population.[7–9] Color Doppler diagnosis of torsion is based on a subjective impression of unilaterally diminished testicular perfusion. However, in the prepubertal population in particular, normal testicular flow is depicted with difficulty. A noninvasive diagnostic method capable of providing quantitative measurement of tissue oxygenation rather than a qualitative assessment of relative testicular perfusion as provided by color Doppler US would be ideal for evaluating patients with acute scrotal symptoms and assessing testicular viability after detorsion. Given the potential risks of anesthesia and surgery, an added benefit would be the avoidance of emergency exploration in patients with nonviable testes.

There is a perceived need by the pediatric urological community for improved noninvasive methods for the diagnosis of testicular torsion, particularly in the pediatric population. In February 2005, the National Institute of Diabetes and Digestive and Kidney Diseases (NIDDK) of the National Institutes of Health (NIH) sponsored a workshop to evaluate the state of research in the field of pediatric urology and to formulate a strategic plan for the future. With respect to testicular torsion, it was noted that current diagnostic methods are imperfect, and that "research addressing alternative strategies for diagnosis is greatly needed."[10]

NIRS has been previously proposed for imaging human testes with an envisioned application of testicular tumor detection,[11] and it has been used to assess testicular hemodynamics and oxygenation in a boar model based on the occlusion of the spermatic vessel or the vas deference with its vessels[12] and in a sheep model of testicular torsion.[13] The boar study showed the capability of NIRS in detecting the effects of vascular occlusions in testes through relative measurements of active testicular blood volume (ATBV). Specifically, in their boar study, Colier et al. found no measurable ATBV after occlusion of the spermatic vessels, suggesting subsequent atrophy.[12] In this boar study, NIRS measurements of active testicular blood volume required a transient lowering of arterial saturation by reducing the fraction of inspired oxygen for a few minutes. The sheep study[13] investigated the absolute tissue saturation (StO_2) of testes at baseline, and following 720-deg torsion (on one side) or sham surgery (on the other side), similar to the protocol reported in our study. NIRS measurements were performed every 15 min with a single source-detector distance, continuous wave spectrometer that allowed for absolute tissue saturation measurements. The results of the sheep study found a median baseline tissue saturation of 59% (interquartile range 57 to 69%) on the experimental side and 67% (interquartile range 59 to 68%) on the control side.[13] About 2.5 h after torsion surgery, the torsioned testes stabilized to a lower median tissue saturation value of 14% (interquartile range 11 to 29%), whereas the sham surgery testes showed[13] an increased median tissue saturation of 77% (interquartile range 77 to 94%).

Our study was conducted on rabbit's testes, whose size compare well to those found in the pediatric population. In contrast to the boar and sheep studies already mentioned, we used a multidistance, frequency-domain NIRS approach to quantifying the absolute concentration and saturation of hemoglobin in testicular tissue. This approach separately measures the absorption and reduced scattering coefficients of tissue, and translates the absorption coefficients at two wavelengths (690 and 830 nm in this study) into absolute concentration and saturation of hemoglobin.

2 Experimental Methods

2.1 *Selection of Animals*

The study was performed according to a protocol approved by the Animal Care and Use Committee of Children's Hospital Boston, Boston, Massachusetts, and conformed to guidelines issued by the NIH for care of laboratory animals. Use of the rabbit in experimental models of testicular ischemia is well established.[14–16] Four adult male New Zealand white rabbits (Millbrook Breeding Labs, Amherst, Massachusetts) with a mean weight of 4.0 kg were examined.

2.2 *Animal Preparation*

General anesthesia was induced with glycopyrrolate 0.04 mg/kg IM (intramuscular), followed by ketamine 10 mg/kg IV (intravenous), and acepromazine 0.5 mg/kg IV. Endotracheal intubation was performed, and the animals placed on a ventilator. Anesthesia was maintained with 0.25 to 3% isoflurane. A catheter was placed in one ear vein of each experimental animal for administration of maintenance fluids. A heparin flush was placed on the venous line. For pain control prior to scrotal incision and testicular torsion, a spermatic cord block was administered containing bupivacaine/lidocaine ($\leqslant$3 mg/kg total dose) and a dose of ketoprofen (1 mg/kg) IM. At the conclusion of the experiment, each rabbit was sacrificed with an intravenous overdose of pentobarbital (1 mL/4.5 kg).

2.3 *Surgical Procedure*

Bilateral medial, ventral incisions were made under sterile conditions and the scrotal layers dissected to the tunica vaginalis. The testes were exposed, and following unilateral torsion and contralateral orchidopexy (sham surgery) the testes were secured in place and the overlying scrotum closed. Sham surgery follows the same exact protocol as the torsion surgery except the twisting of the testis. It involves the opening of the scrotum, manipulation of the testis (remove and replace) and then stitching of the scrotum. Through this protocol, we maintained the surgical conditions so that the postoperative sequel is the same for both sham and torsion surgery, and this enables meaningful measurements of differences between testes that underwent torsion and sham surgeries, respectively.

Baseline NIRS measurements of testicular oxygen saturation levels were obtained followed by unilateral testicular torsions of 720 deg (two twists) in rabbits 1 and 3; 540 deg (one and a half twists) in rabbit 2; 0 deg (same as sham surgery) in rabbit 4 on the experimental testis and contralateral sham surgery on the control testis. Sham surgery on the experimental side was referred to as 0-deg torsion due to the terminology associated with the clinical protocol.

2.4 *Near-IR Tissue Oximeter*

The near-IR experiments were performed using one fiber-coupled photomultiplier tube (PMT) detector and two fiber-coupled laser diodes, one emitting at 690 nm and the other at 830 nm (typical wavelengths used in near-IR tissue oximetry)

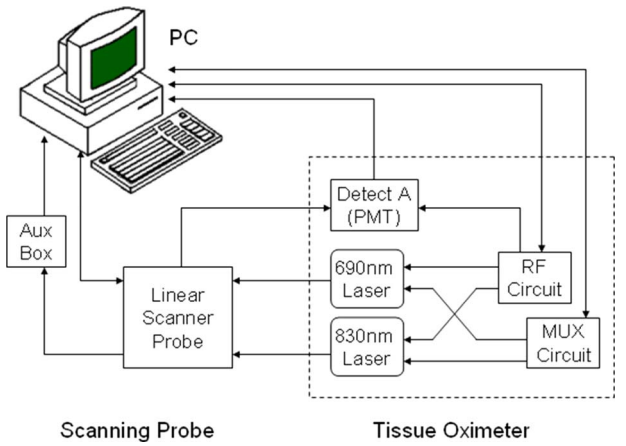

Fig. 1 Experimental setup. The NIRS tissue oximeter (OxiplexTS, ISS, Inc., Champaign, Illinois) houses two laser diodes (emitting at 690 and 830 nm) driven by a radiofrequency (rf) circuit and a multiplexing (MUX) circuit, and one photomultiplier tube (PMT) detector. The specially designed linear scanner probe performs a linear scan of the illumination optical fibers that is synchronized with NIRS acquisition by an auxiliary input box (Aux Box).

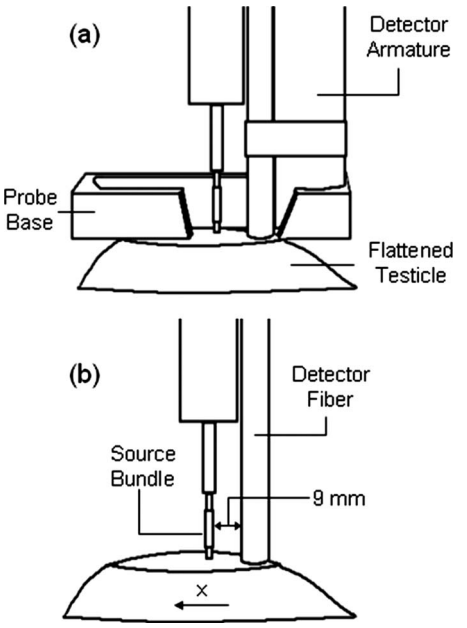

Fig. 2 Configuration of the specially designed optical probe, showing (a) a schematic diagram of the probe including the flattening base and (b) a dissected image of the probe showing the scanning path (along the *x* axis) and an initial (shortest) source-detector distance of 9 mm.

from an OxiplexTS (ISS, Inc., Champaign, Illinois) optical tissue spectrometer.[4] This is a frequency-domain instrument operating at a modulation frequency of 110 MHz. Light was delivered to and from the tissue by a pair of single illumination fibers, 400 μm in diameter, and by one 3.0-mm-diam detector optical fiber bundle. The two source fibers carrying light at 690 and 830 nm were bundled together and positioned right next to each other at the emission end. A programmable mechanical linear stage (Model XN10-0020-M01-71, Velmex, Inc., Bloomfield, New York) was used for linear scanning of the two illumination fibers toward and away from the fixed collection fiber bundle over each testis. Figure 1 shows the experimental setup.

2.5 *Data Acquisition*

Multidistance, frequency-domain measurements were performed on each testis, with a fixed detector and a linearly scanned dual-wavelength source. Figure 2 illustrates the probe placement and scanning method. The detector fiber was placed in contact with the tissue at the inferior aspect of the scrotum and the source pair of illumination fibers was placed at a distance of ~1 mm from the tissue and at an initial distance of approximately 9 mm from the detector fiber. We performed a linear scan of the source pair along the *x* coordinate over the gently flattened scrotal surface covering a source-detector distance range of ~9 to ~18 mm. During the linear scan we acquired frequency-domain measurements of amplitude (ac) and phase (Φ). The linear scan was performed back and forth (i.e., along $+\hat{\mathbf{x}}$ and $-\hat{\mathbf{x}}$) in "sweeps" (each unidirectional scan) multiple times in a continuous manner. An ideal measurement method would be to register the beginning and end of each scan within the oximeter; however, due to hardware limitations such as the maximum data acquisition rate of the oximeter and the minimum scan speed of the linear stage, this was not a possible option in this work. Instead, source fiber positions and NIRS measurements were logged separately, and the linear scanner was setup to generate a trigger signal that was transmitted through an auxiliary connection (Fig. 1) to the computer and registered by the NIRS instrument for synchronization purposes. An average scanning speed of ~2.6 mm/s was used, while optical measurements were taken at a data acquisition rate of 25 Hz. Two sets of optical properties (one set at 690 nm and one set at 830 nm) were obtained through each sweep. Each sweep was followed by a ~5-s pause (that brought scanning motors to a complete stop) to help separate the continuous scans and set the experimental parameters to default before each scan. As a result, we collected one amplitude/phase data point every ~0.1 mm along the scanning coordinate *x*, and one absorption/scattering data point (from each sweep) every ~8 to 9 s. Of course, one can increase the speed of data collection (one single sweep yields a reading of optical coefficients in a few seconds) but for the purposes of this study, aimed at measurements of stable baseline or postsurgery values of hemoglobin concentration and saturation, a time of 8 to 9 s between successive measurements of optical coefficients was appropriate.

2.6 *Data Analysis*

We used the frequency-domain solution to the diffusion equation in the semi-infinite geometry with extrapolated boundary conditions as a model for the optical signal detected in our study.[17] This solution was implemented in an inversion procedure using the Levenberg-Marquardt method[18] to iteratively compute the absolute optical properties (μ_a and μ_s') of the testicular tissue from the amplitude (ac) and phase (Φ) of the detected optical signal. The solution to the diffusion equation we used is

$$\tilde{R}(\rho,\omega)=A\frac{1}{4\pi}\left[z_0\left(\frac{1}{r_1}+\tilde{\mu}_{\text{eff}}\right)\frac{\exp(-r_1\tilde{\mu}_{\text{eff}})}{r_1^2}+(z_0+2z_b)\left(\frac{1}{r_2}+\tilde{\mu}_{\text{eff}}\right)\frac{\exp(-r_2\tilde{\mu}_{\text{eff}})}{r_2^2}\right], \quad (1)$$

where $\tilde{R}$ represents the complex output flux (or reflectance) at source-detector distance ρ and angular modulation frequency ω, so that the measured ac amplitude is given by $\text{ac}=|\tilde{R}(\rho,\omega)|$ and the phase is given by $\Phi=\arg[\tilde{R}(\rho,\omega)]$; $z_0=1/\mu_s'$ (with μ_s' reduced scattering coefficient); r_1^2 and r_2^2 are given, respectively by $r_1^2=z_0^2+\rho^2$ and $r_2^2=(z_0+2z_b)^2+\rho^2$, where z_b is the distance between the real and the extrapolated boundary;[19] $\tilde{\mu}_{\text{eff}}=[(\mu_a c+i\omega)/Dc]^{1/2}$, where c is the speed of light in the medium, and D is the optical diffusion coefficient $[D=1/(3\mu_s')]$; A is an amplitude factor used to match the ac values predicted by the model with those measured. We observe that since the absolute phase shift Φ cannot be experimentally measured, we measured the phase at a generic source-detector distance ρ relative to the phase at the shortest source-detector distance. From the absorption coefficient obtained with this fitting procedure, we calculate the concentrations of oxyhemoglobin $[\text{HbO}_2]$ and deoxyhemoglobin [Hb] in tissue as follows:[4]

$$[\text{HbO}_2]=\frac{\mu_a^{\lambda_1}\varepsilon_{\text{Hb}}^{\lambda_2}-\mu_a^{\lambda_2}\varepsilon_{\text{Hb}}^{\lambda_1}}{\varepsilon_{\text{HbO}_2}^{\lambda_1}\varepsilon_{\text{Hb}}^{\lambda_2}-\varepsilon_{\text{HbO}_2}^{\lambda_2}\varepsilon_{\text{Hb}}^{\lambda_1}}, \quad (2)$$

$$[\text{Hb}]=\frac{\mu_a^{\lambda_2}\varepsilon_{\text{HbO}_2}^{\lambda_1}-\mu_a^{\lambda_1}\varepsilon_{\text{HbO}_2}^{\lambda_2}}{\varepsilon_{\text{HbO}_2}^{\lambda_1}\varepsilon_{\text{Hb}}^{\lambda_2}-\varepsilon_{\text{HbO}_2}^{\lambda_2}\varepsilon_{\text{Hb}}^{\lambda_1}}, \quad (3)$$

where ε_{Hb} and $\varepsilon_{\text{HbO}_2}$ are the molar extinction coefficients of deoxyhemoglobin and oxyhemoglobin (here we have used the following values:[20] $\varepsilon_{\text{Hb}}(690\text{ nm})=4.854\text{ mM}^{-1}\text{ cm}^{-1}$, $\varepsilon_{\text{HbO}_2}(690\text{ nm})=0.956\text{ mM}^{-1}\text{ cm}^{-1}$, $\varepsilon_{\text{Hb}}(830\text{ nm})=1.790\text{ mM}^{-1}\text{ cm}^{-1}$, $\varepsilon_{\text{HbO}_2}(830\text{ nm})=2.333\text{ mM}^{-1}\text{ cm}^{-1}$). Finally, the oxygen saturation of hemoglobin in the tissue (StO_2) is given by[4]

$$\text{StO}_2=\frac{[\text{HbO}_2]}{[\text{HbO}_2]+[\text{Hb}]}. \quad (4)$$

3 Results

In each rabbit we performed sequential measurements on the two sides preoperative and postoperative. Each measurement consisted of about 112 sweeps of the illumination fibers over a total time of about 25 min. Table 1 reports the average values measured over the multiple sweeps for the absorption and reduced scattering coefficients (at both wavelengths), the concentrations of oxyhemoglobin, deoxyhemoglobin, and total hemoglobin, and the tissue hemoglobin saturation for right and left sides, pre- and postoperative, for all four rabbits. The error in each of these measured parameters was estimated by the standard deviation over the multiple sweeps and is reported in Table 1, where the error in the last significant digit is indicated in parenthesis. Such standard deviation over the multiple sweeps, as opposed to the standard error (i.e., the standard deviation divided by the square root of the number of sweeps), gives an estimate of the error on a single measurement, which is the case of a practical clinical measurement.

At baseline and after sham surgery, the absorption coefficients at 690 nm are smaller than those at 830 nm, which is consistent with high values of hemoglobin saturation ($>65\%$). By contrast, after torsion surgery the absorption coefficients at 690 nm are greater than those at 830 nm, which is indicative of low values of hemoglobin saturation ($<40\%$). Such dramatic wavelength-dependent changes observed in the measured absorption coefficients after torsion surgery are not reflected in similar or correlated changes in the reduced scattering coefficients, which always show smaller values at the longer wavelength, as expected for the case of optically turbid media such as tissues. In fact, the normalized differences of the optical coefficients at the two wavelengths {i.e., $[\mu(690\text{ nm})-\mu(830\text{ nm})]/[\mu(690\text{ nm})+\mu(830\text{ nm})]$, where μ is either the absorption or reduced scattering coefficient} show a change between post- and pretorsion surgery of 0.40 ± 0.08 for absorption (significantly different from zero: $p<0.02$) and 0.05 ± 0.04 for reduced scattering (not significantly different from zero: $p>0.1$).

The measured values of [Hb] and $[\text{HbO}_2]$ tissue concentrations before and after surgery are reported graphically in Fig. 3, while the absolute values of tissue oxygen saturation before and after surgery are shown in Fig. 4. The main results reported in Figs. 3 and 4 are the following:

1. The absolute baseline (preoperative) values of [Hb], $[\text{HbO}_2]$, and StO_2 are consistent across animals with average $\pm$ standard deviation values of 17 ± 3 μM for baseline [Hb], 62 ± 13 μM for baseline $[\text{HbO}_2]$, and $78\%\pm5\%$ for baseline StO_2.
2. The absolute values of [Hb], $[\text{HbO}_2]$, and StO_2 after sham surgery are consistent across animals with average $\pm$ standard deviation values of 25 ± 7 μM for [Hb], 86 ± 30 μM for $[\text{HbO}_2]$, and $77\%\pm6\%$ for StO_2.
3. The absolute values of [Hb], $[\text{HbO}_2]$, and StO_2 after torsion surgery are consistent across animals with average $\pm$ standard deviation values of 54 ± 7 μM for baseline [Hb], 31 ± 3 μM for baseline $[\text{HbO}_2]$, and $36\%\pm2\%$ for baseline StO_2.
4. As a result of our absolute measurements at baseline, after sham, and after torsion surgery, we found that the changes in [Hb], $[\text{HbO}_2]$, and StO_2 in response to sham surgery ($\Delta[\text{Hb}]^{(\text{sham})}=7\pm9$ μM, $\Delta[\text{HbO}_2]^{(\text{sham})}=27\pm32$ μM, $\Delta\text{StO}_2^{(\text{sham})}=0\%\pm8\%$) are significantly different from the changes in response to torsion surgery ($\Delta[\text{Hb}]^{(\text{torsion})}=38\pm11$ μM, $\Delta[\text{HbO}_2]^{(\text{torsion})}=-34\pm17$ μM, $\Delta\text{StO}_2^{(\text{torsion})}=-44\%\pm5\%$).

The strong testicular tissue desaturation measured in response to torsion surgery, and the consistent absolute values of hemoglobin concentration and saturation across animals are the major results of this study.

4 Discussion

The absolute measurement capability of the frequency-domain approach to near-IR oximetry employed in this study is a feature of paramount importance. In fact, a reliable assessment of tissue viability in a clinical setting may not al-

Table 1 Mean absolute values of the optical properties [absorption coefficient (μ_a) and reduced scattering coefficient (μ_s')] at 690 and 830 nm, hemoglobin concentrations (oxyhemoglobin [HbO_2], deoxyhemoglobin [Hb], total hemoglobin [*t*Hb]), and hemoglobin saturation (StO_2) measured on the right and left testes of the four rabbits included in this study. The error in the last significant digit is reported in parenthesis and represents the standard deviation of the measurements over multiple scans.

Rabbit No	Testis Side	Surgical Stage	μ_a 690 nm (cm^{-1})	μ_a 830 nm (cm^{-1})	μ_s' 690 nm (cm^{-1})	μ_s' 830 nm (cm^{-1})	[HbO_2] (μM)	[Hb] (μM)	[*t*Hb] (μM)	StO_2 (%)
1	Left	Baseline	0.16(1)	0.21(2)	6.0(3)	5.6(4)	73(10)	19(2)	92(12)	79(2)
		Control	0.19(1)	0.19(1)	6.8(4)	5.6(3)	57(8)	27(4)	84(11)	67(5)
	Right	Baseline	0.18(2)	0.22(3)	5.3(3)	4.9(4)	79(14)	21(3)	100(17)	79(3)
		Torsion—720 deg	0.26(2)	0.15(1)	6.1(3)	5.2(2)	30(6)	47(4)	77(10)	39(6)
2	Left	Baseline	0.12(1)	0.18(2)	5.9(1)	5.4(3)	68(9)	12(2)	80(11)	84(3)
		Torsion—540 deg	0.29(4)	0.16(3)	5.6(3)	4.2(6)	30(10)	53(8)	83(18)	35(8)
	Right	Baseline	0.17(1)	0.20(2)	5.5(1)	4.9(3)	68(10)	22(2)	90(13)	76(4)
		Control	0.18(3)	0.23(3)	5.8(4)	5.1(6)	84(15)	20(5)	103(20)	81(4)
3	Left	Baseline	0.12(1)	0.14(1)	3.9(3)	3.5(4)	49(7)	14(2)	64(9)	78(4)
		Torsion—720 deg	0.33(2)	0.19(1)	8.1(7)	7.0(3)	34(8)	62(6)	96(14)	36(7)
	Right	Baseline	0.12(0)	0.12(1)	4.7(1)	3.8(2)	38(3)	18(1)	56(5)	68(3)
		Control	0.14(2)	0.16(4)	4.1(4)	3.7(4)	57(12)	17(8)	73(21)	77(4)
4	Left	Baseline	0.13(1)	0.17(1)	4.6(1)	4.0(2)	59(5)	16(1)	75(7)	79(2)
		Control	0.29(1)	0.35(4)	3.0(7)	3.0(3)	125(7)	35(2)	160(9)	78(2)
	Right	Baseline	0.12(1)	0.16(1)	4.7(3)	3.8(3)	57(7)	13(2)	70(9)	81(4)
		Torsion—0 deg	0.22(2)	0.29(2)	3.1(2)	3.0(1)	106(8)	25(4)	131(12)	81(3)

ways be based on relative measurements of changes induced by a diagnostic procedure. In the specific case of testicular viability assessment, which is the focus of this study, the question is how values of hemoglobin saturation in pathologic testes compare with the range of saturation values measured on healthy testes. Even though our study involves a relatively small number of animals (four), it nevertheless provides strong indications on this point. In fact, the absolute values of tissue hemoglobin saturation measured on torsioned testes ($36\% \pm 2\%$, $n=3$) is significantly different from the saturation values measured at baseline, after sham surgery, or after 0-deg torsion surgery ($77\% \pm 5\%$, $n=13$) ($p<0.0001$). As a result, one can hypothesize that absolute oxygenation measurements can successfully assess testicular viability for the diagnosis of testicular torsion and monitoring of therapy without relying on a comparison with reference or baseline data. Here we stress again that the errors on the oxygen saturation measurements are the standard deviations of the measurements over multiple sweeps, so that they provide indications of errors on a single measurement, which is relevant for prospective clinical applications of the method.

We observe that the relatively small variability of 5 to 6% (standard deviation) in the tissue hemoglobin saturation (StO_2) measured across animals at baseline (presurgery) and after sham surgery demonstrates the relative insensitivity of StO_2 to a number of factors that may potentially confound NIRS measurements. Such factors include tissue heterogeneity, changes in temperature and blood pressure of the animal, and vascular changes induced by sham surgery. Furthermore, physical effects such as the changes in testicular structure and presence of sutures after surgery may also potentially introduce artifacts or unwanted contributions to optical measurements. However, despite the many potentially confounding factors introduced by surgery, our absolute measurements are highly consistent, especially those for StO_2, so that we have been able to robustly differentiate the effects of sham surgery and torsion surgery from StO_2 measurements.

The results of our rabbit study confirm the feasibility of measuring testicular deoxygenation with NIRS, as previously reported in a boar study by Colier et al.[12] and in a sheep study by Capraro et al.[13] These previous studies have used continuous-wave NIRS, and obtained absolute measurements of testicular hemoglobin saturation by introducing a blood oxygenation bolus (boar study) or some kind of calibration (sheep study). Our approach to the absolute measurement of the concentration and saturation of hemoglobin in testicular tissue is based[21] on multidistance, frequency-domain NIRS, in conjunction with the solution to the diffusion equation in

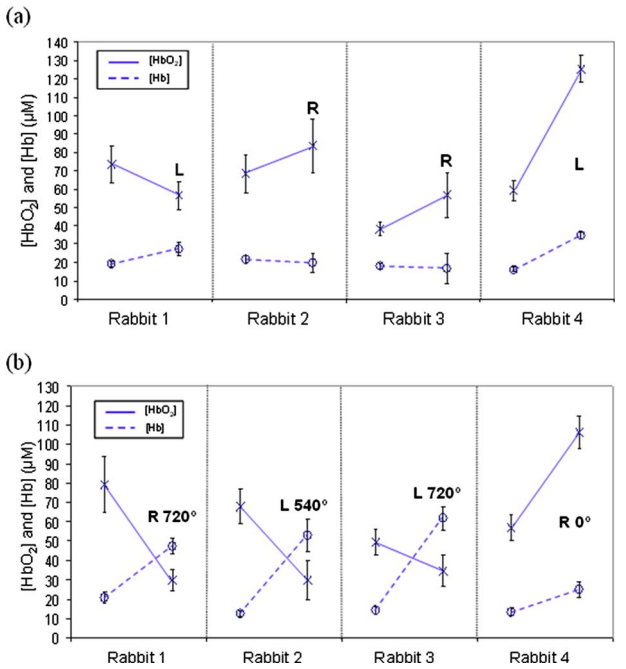

Fig. 3 Absolute values of concentrations of HbO_2 and Hb measured in testicular tissue for all four rabbits. Each line starts at the baseline value and ends at the postoperative value of $[HbO_2]$ (continuous lines) and [Hb] (dashed lines) on (a) the control testes or (b) the experimental testes. Here *L* refers to left and *R* refers to right testicle with associated degrees of torsions.

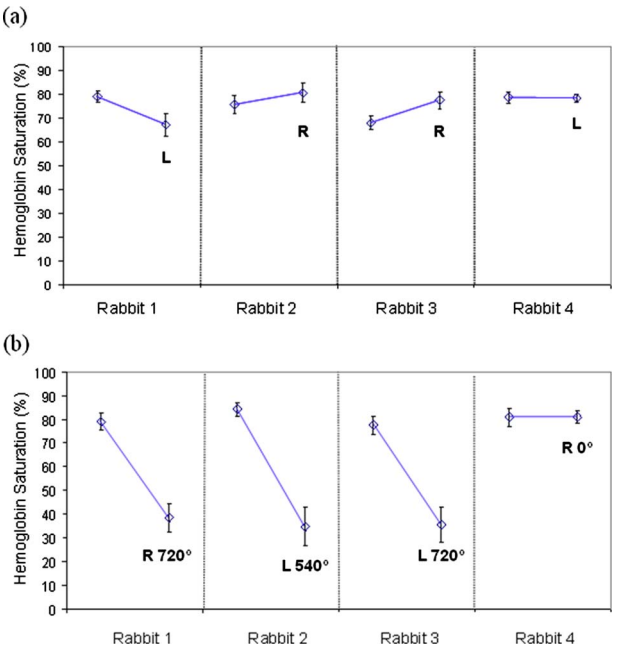

Fig. 4 Absolute hemoglobin saturation values measured in the testicular tissue for all four rabbits. Each line starts at the baseline value and ends at the postoperative value of tissue hemoglobin saturation on (a) the control testes or (b) the experimental testes. Here *L* refers to left and *R* refers to right testicle with associated degrees of torsions.

semi-infinite geometry given by Eq. (1). The assumptions associated with the use of this solution are tissue homogeneity (so that the measured hemoglobin parameters are spatial averages over the probed volume), the applicability of diffusion theory (which is expected to be appropriate for highly scattering tissues at source-detector distances >0.8 cm), and semi-infinite boundary conditions for the tissue under investigation. While these assumptions are not strictly satisfied by measurements of tissues *in vivo*, the reproducibility of the concentration and saturation values found in this study, together with their physiological plausibility, give confidence in the validity of the assumptions. In particular, we note that the use of idealized semi-infinite boundary conditions to describe light propagation in relatively small tissue volumes (average size of testes: $3\times1.5\times1$ cm, length, width, depth) affects mainly the absolute values of the absorption coefficients retrieved by the fitting procedure. Monte Carlo simulations on finite tissue volumes of similar sizes of the testicles (not reported in this paper) showed that using semi-infinite boundary conditions led to overestimation of the absorption coefficient but hemoglobin saturation calculations were always within 2 to 3% of the correct values.

5 Conclusion

We showed that a multidistance NIRS technique is capable of providing an absolute measure of testicular parenchymal oxygenation and concentration of hemoglobin, and distinguishing a normal testis from a torsive testis in an experimental rabbit model. These promising data justify further investigation of this technique in a clinical trial with the possibility of providing a more accurate assessment of acute testicular pain in the pediatric population than has been possible with currently available diagnostic tools.

Acknowledgments

This research was supported by a CIMIT New Concept Award funded by U.S. Army Acquisition Activity, Cooperative Agreement W81XWH-09-2-0011.

References

1. E. Gratton and S. Fantini, "Reflectance and transmittance spectroscopy," Chap. 11 in *Lasers and Current Optical Techniques in Biology*, Comprehensive Series in Photochemistry and Photobiology, Vol. **4**, G. Palumbo, R. Pratesi, Eds., pp. 211–258, Royal Chemistry, Cambridge, UK (2004).
2. E. Gratton, S. Fantini, M. A. Franceschini, and M. Fabiani, "Measurements of scattering and absorption changes in muscle and brain," *Philos. Trans. R. Soc. London* **352**(1354), 727–735 (1997).
3. S. Fantini, M. A. Franceschini, J. Maier, S. Walker, B. Barbieri, and E. Gratton, "Frequency-domain multichannel optical detector for noninvasive tissue spectroscopy and oximetry," *Opt. Eng.* **34**(1), 32–42 (1995).
4. S. Fantini and M. A. Franceschini, "Frequency-domain techniques for tissue spectroscopy and imaging," Chap. 7 in *Handbook of Optical Biomedical Diagnostics*, V. V. Tuchin, Ed., pp. 405–453, SPIE Press, Bellingham, WA (2002).
5. R. C. N. Williamson, "Torsion of the testis and allied conditions," *Br. J. Surg.* **63**(6), 465–476 (1976).
6. K. B. H. Koh, N. Dublin, and T. Light, "Testicular torsion," *ANZ J. Surg.* **65**(9), 645–646 (1995).
7. A. R. Blask, D. Bulas, S.-R. Eglal, G. Rushton, C. Shao, and M. Majd, "Color Doppler sonography and scintigraphy of the testis: a prospective, comparative analysis in children with acute scrotal pain," *Pediatr. Emerg. Care* **18**(2), 67–71 (2002).

8. N. Kalfa, C. Veyrac, C. Baud, A. Couture, M. Averous, and R. B. Galifer, "Ultrasonography of the spermatic cord in children with testicular torsion: impact on the surgical strategy," *J. Urol. (Baltimore)* **172**(4), 1692–1695 (2004).
9. B. Karmazyn, R. Steinberg, L. Kornreich, E. Freud, S. Grozovski, M. Schwarz, N. Ziv, and P. Livne, "Clinical and sonographic criteria of acute scrotum in children: a retrospective study of 172 boys," *Pediatr. Radiol.* **35**(3), 302–310 (2005).
10. NIDKK, "Other pediatric urinary conditions," Chap. 3 in *NIDKK Research Progress Report and Strategic Plan for Pediatric Urology*, pp. 57–65 (2006).
11. U. Hampel, E. Schleicher, and R. Freyer, "Volume image reconstruction for diffuse optical tomography," *Appl. Opt.* **41**(19), 3816–3826 (2002).
12. W. Colier, F. Froeling, J. De Vries, and B. Oeseburg, "Measurement of the blood supply to the abdominal testis by means of near infrared spectroscopy," *Eur. Urol.* **27**(2), 160–166 (1995).
13. G. Capraro, T. Mader, B. Coughlin, and H. Smithline, "Feasibility of using near-infrared spectroscopy to diagnose testicular torsion: an experimental study in sheep," *Ann. Emerg. Med.* **49**(4), 520–525 (2007).
14. D. P. Frush, D. S. Babcock, A. G. Lewis, H. J. Paltiel, R. Rupich, K. E. Bove, and C. A. Sheldon, "Comparison of color Doppler sonography and radionuclide imaging in different degrees of torsion in rabbit testes," *Acad. Radiol.* **2**(11), 945–951 (1995).
15. S. M. O'Hara, D. P. Frush, D. S. Babcock, A. G. Lewis, L. L. Barr, T. P. Bukowski, B. M. Kline-Fath, and C. A. Sheldon, "Doppler contrast sonography for detecting reduced perfusion in experimental ischemia of prepubertal rabbit testes," *Acad. Radiol.* **3**(4), 319–324 (1996).
16. B. D. Coley, D. P. Frush, D. S. Babcock, S. M. O'Hara, A. G. Lewis, M. J. Gelfand, K. E. Bove, and C. A. Sheldon, "Acute testicular torsion: comparison of unenhanced and contrast-enhanced power Doppler US, color Doppler US, and radionuclide imaging," *Radiology* **199**(2), 441–446 (1996).
17. S. Fantini, M. A. Franceschini, and Enrico Gratton, "Semi-infinite-geometry boundary problem for light migration in highly scattering media: a frequency-domain study in the diffusion approximation," *J. Opt. Soc. Am.* **11**(10), 2128–2138 (1994).
18. W. H. Press, S. A. Teukolsky, W. T. Vetterling, and B. P. Flannery, "Numerical recipes," in *Numerical Recipes in FORTRAN 77*, 2nd ed., *The Art of Scientific Computing*, Cambridge University Press, Cambridge, U.K. (1992).
19. D. Contini, F. Martelli, and G. Zaccanti, "Photon migration through a turbid slab described by a model based on diffusion approximation. I. Theory," *Appl. Opt.* **36**(19), 4587–4599 (1997).
20. S. Wray, M. Cope, D. T. Delpy, J. S. Wyatt, and E. O. R. Reynolds, "Characterisation of the near infrared absorption spectra of cytochrome aa3 and haemoglobin for the non-invasive monitoring of cerebral oxygenation," *Biochim. Biophys. Acta* **933**(1), 184–192 (1988).
21. S. Fantini, M. A. Franceschini, J. B. Fishkin, B. Barbieri, and E. Gratton, "Quantitative determination of the absorption spectra of chromophores in strongly scattering media: a light-emitting-diode based technique," *Appl. Opt.* **33**(22), 5204–5213 (1994).